

# Phase Unwrapping and Background Correction in MRI

Tian Lan, Deniz Erdogmus, *Senior Member, IEEE*, Susan J Hayflick, J. Urick Szumowski

**Abstract**—Magnetic Resonance Imaging (MRI) has been widely used for both clinical diagnostics and in-vivo research. Although MRI images are acquired in the complex number field, traditionally magnitude images are utilized for most applications, while the phase of the complex numbers is ignored due to various signal processing and visualization issues. However, there is substantial evidence that a phase of MRI image can contain additional useful diagnostic information. For example the phase of MRI image can be used to detect excessive iron accumulation associated with many neurodegenerative disorders such as Alzheimer’s and Parkinson disease. Phase wrapping and background phase variations are two main problems, which prevent clinical use of phase images directly. In this paper, we propose 2-D technique for phase unwrapping and background phase correction based on spectral image segmentation and detrending algorithms. This method handles various noise levels successfully, and most importantly, its extension to 3-D volumetric MRI phase image processing is conceptually straightforward.

## I. INTRODUCTION

Magnetic Resonance Imaging (MRI) has revolutionized clinical practice through its noninvasive imaging capabilities. The MRI is acquired as a complex-valued signal, however magnitude images are traditionally utilized, while phase images are largely ignored and discarded due to various difficulties in processing and visualizing them. It is known from Fourier analysis of signals that the phase of a complex number carries significant information and recently more researchers are realizing that in MRI useful information can be extracted from the phase data.

The measured phase is normally wrapped onto the range of  $[-\pi, +\pi]$ , which does not reflect the true relative phase values across space as seen in Figure 1. Thus phase unwrapping is required before visualization or further processing. Phase unwrapping in one dimension is a trivial problem; however, in higher dimensionalities, it is computational intensive and noise sensitive. There are many 2D phase unwrapping algorithms in the literature, most of which can be categorized as either branch-cut or weighted least-square methods [3-6]. Chiglia and Romero proposed the minimum  $L^0$ -norm solution, which connects two types of

methods [7]. These methods do solve the 2D phase unwrapping problem, but they are not easy to expand to 3D. Furthermore, these methods are either path-dependent or they easily get trapped in local minima. Huntley developed a 3D noise-immune unwrapping algorithm by extending a branch-cut type 2D approach [8]. Although this path-independent algorithm has less ambiguity, the pixel based unwrapping procedure exhibits low efficiency.

Another problem of phase images is the background phase variations due to the magnetic field inhomogeneities across an MRI image (see Figure 4a later in the text). Usually, the background phase has slowly varying spatial characteristics while the signals of interest that relate to e.g. iron concentrations in tissue have relatively high frequency content. Intuitively, one needs a suitable highpass filter design to remove the background phase variations (after phase unwrapping). However, in many cases, the background phase shift and the ‘true’ signal phase overlap in frequency domain, thus linear highpass filters fail to achieve optimal separation. Moreover, designing the cut-off frequency for such filters is typically heuristic; hence generalization of performance to different images is nontrivial.

In this paper, we propose a nonparametric nonlinear method for solving these two problems, namely phase unwrapping and background subtraction. Specifically, we develop (i) a region based branch-cut algorithm for phase unwrapping, and (ii) a region based kernel regression approach for background phase variations correction. These two parts of the technique are applied sequentially to phase images. Suitable image segmentation techniques based on different criteria are employed for the two parts. Phase unwrapping is achieved by utilizing pixel-coordinate and phase-value as features in conjunction with a specifically designed wrapping kernel for pairwise affinity based clustering; after over-segmentation with this technique, a segment-neighborhood graph is formed and segments are merged as the phase unwrapping is achieved by adding an appropriate integer multiple of  $2\pi$  and updating the neighborhood graph by merging the nodes corresponding to the phase-aligned segments. This procedure is repeated until all segments are merged (single node is left in the graph). This method does not rely on a specific path; the phases of neighboring regions are corrected simultaneously, therefore it is more efficient compared to pixel-based unwrapping algorithms. Next, background phase correction is achieved by segmenting relatively high-frequency peaks using the mean-shift procedure on position-phase features and estimating/interpolating the background under the region of

This work was partially supported by NSF under grants ECS-0524835, ECS-0622239, and IIS-0713690 and also by the NBIA Disorders Association and by the National Organization for Rare Disorders.

Tian Lan and Deniz Erdogmus are with the Biomedical Engineering Department, Oregon Health and Science University, Portland, OR 97006 USA. (contact email: derdogmus@ieee.org)

Susan J Hayflick is with the Department of Molecular and Medical Genetics, Oregon Health and Science University, Portland, OR 97006 USA.

J. Urick Szumowski is with the Department of Radiology, Oregon Health and Science University, Portland, OR 97006 USA.

interest by obtaining a kernel regression solution from the region surrounding the hole generated by removing the segment containing the desired phase signal and subtracting it from the region of interest (see Figure 4b in the text).

The technique is easily extendable to 3D MRI processing since it utilizes general nonparametric techniques operating in feature-space rather than the image-directly. Experiments with MRI phase data demonstrate the effectiveness of the proposed approach.

## II. METHOD

A block diagram of the proposed method for phase unwrapping and background subtraction is provided in Figure 2. Next, we describe the details of the algorithm. We will focus our discussion on brain MRI, but the techniques apply to images of other organs.

### A. Phase Unwrapping

*Mask generating:* A brain MRI contains other physically separate objects that are not of interest, such as the skull and empty space around the head. These regions contain irrelevant image pixels that will not only increase the computational load, but also decrease the performance of the any image processing algorithm due to high nonuniformity of phase across and along boundaries. A mask that separates the brain is necessary before any further processing. The mask is generated from the corresponding magnitude image instead of phase image. Specifically, we apply a threshold on the magnitude assuming empty space yields small-magnitude values:

$$M_i = \begin{cases} 1 & I_i \geq th \\ 0 & I_i < th \end{cases} \quad (1)$$

$M$  is the mask image, which contains binary values, 1 means brain, 0 means non-brain.  $I$  is the amplitude,  $i$  is pixel index,  $th$  is the threshold which is acquired from the histogram of pixel magnitudes. The mask is smoothed using a floodfill technique [9] using the *imfill* function in Matlab® in order to eliminate small holes in the mask that occur sporadically throughout the image.

*Spectral clustering algorithm for image segmentation:* Spectral methods have been extensively studied and widely used for dimensionality reduction and clustering [10,11]. Spectral clustering algorithms are special cases of pairwise affinity-based clustering, and they map data represented in the form of feature vectors to the  $k$ -dimensional space spanned by the normalized eigenvectors of the affinity matrix, which corresponding to the  $k$  largest eigenvalues, hence divides the data/image into  $k$  clusters. Determining the number of clusters is a challenging problem. For our specific purpose, we revise the spectral clustering algorithm so that we do need to know  $k$  before hand. We repeat the procedure till we partition all pixels of the image. The algorithm specifically exploits two facts about phase wrapping boundaries – the average phase difference along such a boundary is  $2\pi$  and the segments must consist of connected sets of pixels. Consequently, a kernel that is rectangular

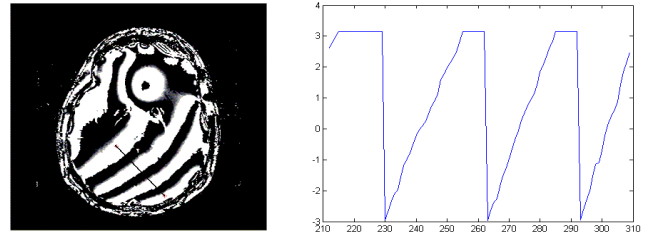


Figure 1. A sample MRI slice that demonstrates phase wrapping (left) and the profile of phase along the line segment shown (right).

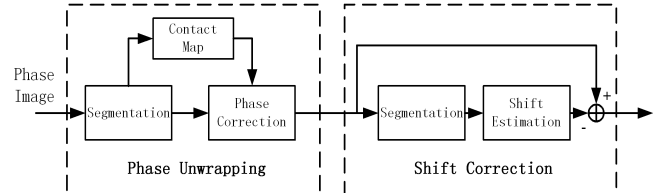


Figure 2. Block diagram of the proposed phase unwrapping and background variations correction approach.

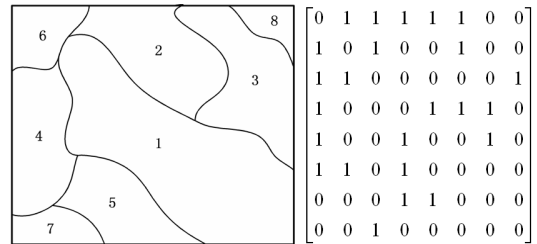


Figure 3. An illustration of the contact map and the contact matrix for a hypothetical phase image segmentation outcome.

uniform on a  $3 \times 3$  pixel region times a mod- $2\pi$  uniform along phase value with support  $\pi$  is employed. This kernel yields an idealized sparse connectivity graph for pixels. The algorithm is as follows:

1. Calculate affinity matrix  $\mathbf{A}=[A_{ij}]$  with  $A_{ij}=K(\mathbf{x}_i-\mathbf{x}_j)$ , where  $\mathbf{x}$  is a 4-dimensional vector containing row and column indices, intensity (wrapped phase value), and edge-feature of a pixel.<sup>1</sup>
2. Find the largest eigenvalue and the corresponding eigenvector  $\mathbf{v}$  of the affinity matrix.
3. For the  $i^{\text{th}}$  element in the largest eigenvector, which corresponds to the  $i^{\text{th}}$  pixel, if the value is larger than a threshold, we assign it to the cluster  $C_j$ , where  $j=1,2,\dots$
4. If pixel  $i$  is assigned to cluster  $C_j$  in step 3, set the  $i^{\text{th}}$  row and column of the affinity matrix to 0.
5. Repeat step 2-4, until all elements in affinity matrix are 0.

*Phase unwrapping using branch-cut method:* Our phase unwrapping algorithm uses the branch-cut approach.

<sup>1</sup> Here,  $i$  and  $j$  are the pixel indices and  $K$  is the affinity/kernel function. The joint kernel is the multiplication of 4 univariate rectangular kernels. For position the kernel is 3-pixels-wide, the phase intensity kernel is  $\pi/10$ -wide with a circular (modular) absolute-difference, and the edge-feature kernel is the thresholded binary edge value for each pixel. This kernel leads to a sparse affinity matrix also taking the phase wrapping into account when measuring affinities.

However, unlike most of branch-cut methods in the literature, which form a particular path and correct the phase along this path pixel by pixel, our method unwraps the phase regionally. First, we rank the regions by decreasing number of pixels, which are acquired from image segmentation in the previous subsection and relabel these clusters such that

$$N_1 \geq N_2 \geq N_3 \geq \dots \geq N_j \quad (2)$$

where  $N_i$  is the number of pixels of the  $i$ th (largest) region. We define the Contact Map (neighborhood graph) and the corresponding Contact Matrix (graph connectivity matrix) as illustrated in Figure 3: if regions  $i$  and  $j$  share a common boundary, we say  $i$  and  $j$  are *in contact* and assign 1 to the corresponding element in the Contact Matrix (CM):

$$CM_{ij} = \begin{cases} 1 & i, j \text{ are Contact} \\ 0 & o/w \end{cases} \quad (3)$$

Given the largest region, region 1, we determine the largest region that it has contact with, labeled region  $j$ , and the algorithm corrects the phase of all pixels in region  $j$  by the amount, an integer multiple of  $2\pi$  such that the average phase difference along the boundary of regions 1 and  $j$  is closest to zero. Regions 1 and  $j$  are then merged and all pixels in  $j$  are assigned the label 1. All region labels, contact map, and matrix are updated accordingly. The procedure is then repeated until all regions are merged and all phase wrapping boundaries are brought to an average of zero. By correcting the phase of complete regions that share phase wrapping boundaries simultaneously, this approach reduces computational requirements significantly compared to pixel-based branch-cut methods.

### B. Correction of Background Phase Variations

The most direct way to subtract the background is to apply a highpass filter on the phase image, since the background is a slowly varying signal over space and the signal of interest related to local molecule concentrations exhibits high frequency content. However, by examining the frequency response of the phase image, we find that the background and target signal components significantly overlap in frequency domain. Consequently, simple linear highpass filters fail to correct the background shift. Moreover, the cut-off frequency selection of the highpass filter tends to be heuristic since exact frequency profiles of the two signals are unknown and optimal Wiener filters cannot be designed.

We model the problem as  $x(\mathbf{p})=s(\mathbf{p})+b(\mathbf{p})+n(\mathbf{p})$ , where  $x(\mathbf{p})$  is the measurement,  $s(\mathbf{p})$  is the desired signal,  $b(\mathbf{p})$  is the unwanted additional background component, and  $n(\mathbf{p})$  is the measurement noise at position  $\mathbf{p}$ . A synthetic example of the signal along a line segment through a high iron-concentration region in the brain is presented in Figure 4a. Visual inspection of typical images reveals that the SNR is reasonably high. We first segment the regions which contain the desired signal from the regions that contain only background (Figure 4b), then estimate the background for all regions by fitting a nonlinear model to the data that contains

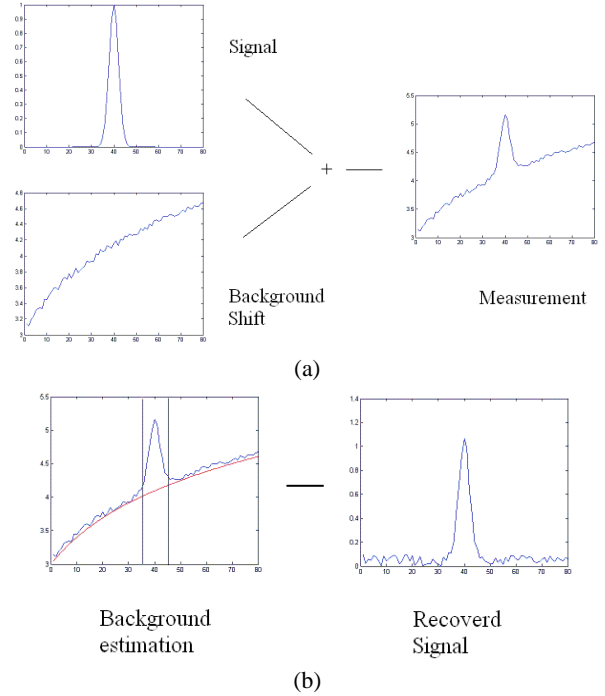


Figure 4. (a) The measurement is composed of the sum of a spatially abrupt desired signal, unknown slowly varying background, and measurement noise. (b) On the left we identify segment boundaries which identify pure-background regions and identifies a nonlinear fit from these segments, and on the right, the desired local phase is extracted after background subtraction.

only background. Finally, we recover the desired signal by subtracting the estimated background from the measurement.

*Mean-shift algorithm for image segmentation:* To separate the unwrapped phase image into the regions which contain the desired signals (often in the form of a sharp *bump*) and the regions which contain only background phase variations, we employ the mean-shift algorithm, an algorithm perfectly suited for this purpose, because it is specifically designed to cluster data based on the existing modes and assigning data to the mode (*bump*) that its gradient ascent trajectory climbs to.

Mean-shift algorithm is a nonparametric clustering technique that does not require prior knowledge of the number of clusters. It finds the modes of density function by moving every sample uphill using fixed-point gradient ascent updates until convergence to local maxima is achieved [12]. Given  $N$  data samples of a  $d$ -dimensional random vector  $\mathbf{x}_i$ ,  $i=1, \dots, N$ , the probability density  $f(\mathbf{x})$  is estimated using kernel density estimation:

$$f(\mathbf{x}) = \frac{1}{N} \sum_{i=1}^N K(\mathbf{x} - \mathbf{x}_i) \quad (4)$$

where  $K(\mathbf{x})$  is a symmetric unimodal kernel function (typically a Gaussian) with an appropriately selected width (typically circular covariance for Gaussian). Taking the derivative of (4) with respect to  $\mathbf{x}$  and equating to zero, for the Gaussian kernel, one obtains the fixed point update:

$$\mathbf{x} \leftarrow \left( \sum_{i=1}^n \mathbf{x}_i G(\mathbf{x} - \mathbf{x}_i) \right) / \left( \sum_{i=1}^n G(\mathbf{x} - \mathbf{x}_i) \right) \quad (5)$$

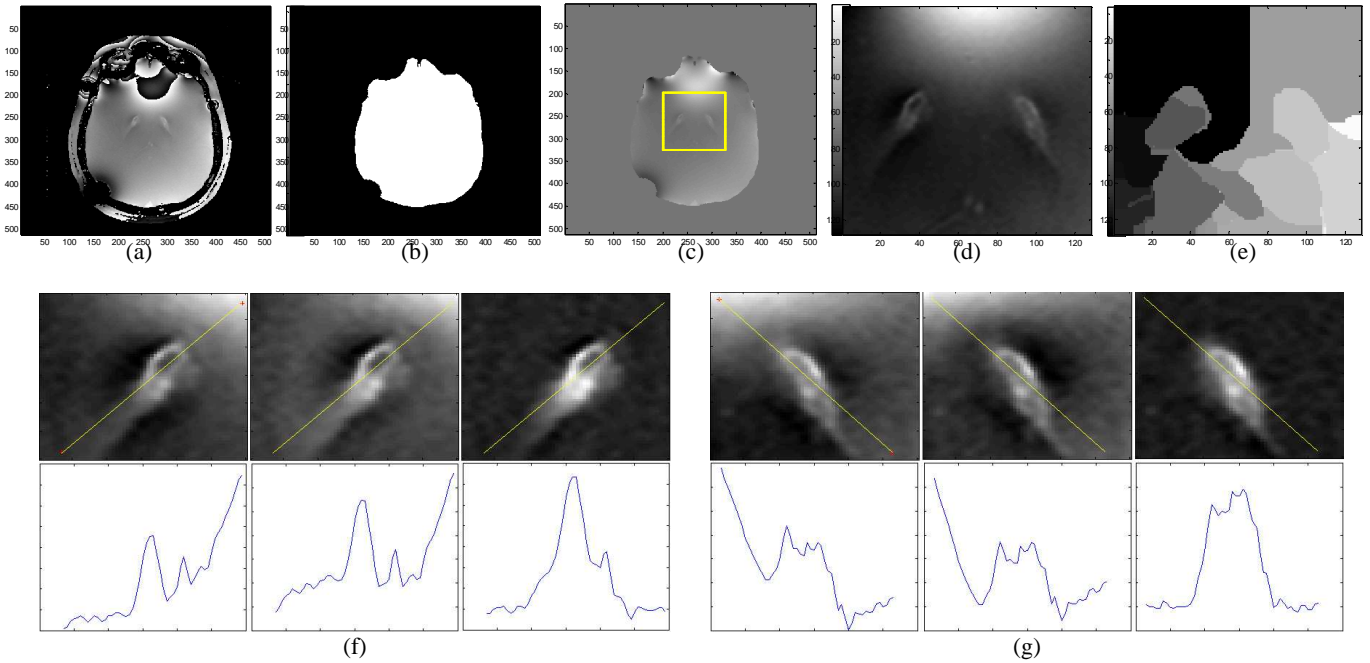


Figure 5. Results of phase unwrapping with correction for background phase variations. (a) Original MRI phase signal; (b) Mask; (c) Unwrapped phase signal inside mask (d) Region of interest; (e) Mean-shift segmentation results of region of interest; (f) Top row: phase around left-hemisphere globus pallidus (left to right) in the original, after highpass filtering, after the proposed processing; bottom row: cross-section of phase along indicated line segment; (g) Top row: phase around right-hemisphere globus pallidus (left to right) in the original, after highpass filtering, after the proposed processing; bottom row: cross-section of phase along indicated line segment.

*Kernel regression for background estimation:* Kernel regression is a nonparametric method for smoothing, curve fitting and denoising [13] and is employed here as a nonparametric nonlinear means of background estimation. Assume that we segment the image into two regions using mean shift followed by merging of all clusters corresponding to the desired signal into one (S) and all background clusters into one (B). The phase value at any pixel coordinate  $\mathbf{p}$  can be represented as:

$$\phi(\mathbf{p}) = \sum_{j=1}^N c_j G(\mathbf{p} - \mathbf{p}_j) \quad (6)$$

where the index  $j$  runs over all pixels in B and,  $G$  is a Gaussian kernel. Using data pairs  $(\mathbf{p}_j, \phi(\mathbf{p}_j))$ , one determines the optimal combination coefficient vector  $\mathbf{c}=[c_1, c_2, \dots, c_N]^T$  as

$$\mathbf{c} = (\mathbf{G} + \lambda \mathbf{I})^{-1} \boldsymbol{\phi} \quad (7)$$

where  $\mathbf{G}$  is the matrix consisting of  $G(\mathbf{p}_i - \mathbf{p}_j)$  in its entries and  $\boldsymbol{\phi}$  is the vector of target phase values at these pixels in B. The regularization parameter  $\lambda$  is introduced to prevent overfitting to noise and is selected by 2-fold cross validation on the pixels in B. Once the optimal  $\mathbf{c}$  is determined, the background estimate in S can be evaluated for pixels in this region using (6) as well.

### III. EXPERIMENTS AND RESULTS

The proposed method is tested on brain MRI phase data. For illustration, we present results obtained on a representative scan. The original phase is shown in Figure 5a in which wrapping is observed near the boundaries of the brain (in many cases wrapping occurs inside the brain as well). The generated mask is shown in Figure 5b and the

unwrapping result for the image portion under the mask is shown in 5c. In this particular case, the phase distortions in the globus pallidus region due to accumulation of iron is of interest and Figure 5d focuses on this region. Mean shift segmentation result of this region is shown in 5e, from which two clusters corresponding to the bump and the background are manually selected by a human expert (only manual action in the procedure at this stage since it is challenging to completely automate the procedure for determining what constitutes a peak of interest and what does not as that requires anatomical and diagnostic knowledge). Figures 5f and 5g present the original phase on the left and right globus pallidus regions as well as results of background correction using the straightforward highpass filtering (with visually optimized cut-off frequency, since there is no ground truth available) and the proposed technique.

### IV. CONCLUSION

In this paper, we proposed a semiautomated technique for MRI phase image unwrapping and correction of background phase variations. The method tackles both unwrapping and background segmentation problems using custom clustering algorithms modified for the particular application. Specifically for phase unwrapping a specific kernel design in conjunction with pixel coordinate and modular-phase intensity difference metric allows the design of a sparse connectivity matrix, thus a straightforward spectral clustering solution. The background segmentation is achieved by mean-shift which specializes in clustering modes/peaks of a distribution function by fixed-point gradient ascent updates.

The main advantages of this method are: (i) phase unwrapping algorithm is based on regions rather than pixels; therefore, it is more effective compared to pixel-based branch cut and least-squares methods; (ii) it is nonparametric, therefore minimal assumptions regarding the image is made hence the technique is versatile; (iii) it is a dimension-independent method and can be easily extended to 3D MRI processing in the same manner. The proposed method has been applied to clinical brain MR phase images for the purpose of isolating iron concentration induced phase distortions in and around the globus pallidus from background fluctuations due to tissue variability. Experimental results showed that the technique effectively unwraps the phase and removes the background phase baseline in comparison to the straightforward highpass filtering approach.

We should note that the performance of segmentation algorithms is critical to the success of the proposed method. Current segmentation algorithms (spectral and mean shift) are computationally very demanding –  $O(N^2)$  for  $N$  pixels. Our future research will focus on improving the speed and efficiency of segmentation without compromising the robustness and accuracy. We will also extend the proposed method to 3D MRI images.

#### REFERENCES

- [1] V. Sehgal, Z. Delproposto, E.M. Haacke, et al., “Clinical Applications of Neuroimaging with Susceptibility-weighted Imaging,” *JMRI*, vol. 22, pp. 439-450, 2005.
- [2] J.H. Duyn, P. van Gelderen, TQ. Li et al, “High Field MRI of Brain Cortical Structure Based on Signal Phase,” *PNAS* vol. 104, pp. 11796, 2007.
- [3] D.C. Ghiglia, L.A. Romero, “Robust Two-dimensional Weighted and Unweighted Phase Unwrapping that Uses Fast Transforms and Iterative Methods,” *J. Opt. Soc. Am. A* vol. 11, pp. 107–117, 1994.
- [4] T.J. Flynn, “Two-dimensional Phase Unwrapping with Minimum Weighted Discontinuity,” *J. Opt. Soc. Am. A*, vol. 14, pp. 2692–2701, 1997.
- [5] C.W. Chen, H.A. Zebker, “Network Approaches to Two-dimensional Phase Unwrapping: Intractability and Two New Algorithms,” *J. Opt. Soc. Am. A*, vol. 17, pp. 401–414, 2000.
- [6] D.C. Ghiglia, M.D. Pritt, *Two-Dimensional Phase Unwrapping*, Wiley, New York, 1998.
- [7] D.C. Ghiglia, L.A. Romero, “Minimum  $L_p$ -norm Two-dimensional Phase Unwrapping,” *J. Opt. Soc. Am. A*, vol. 13, pp. 1999–2013, 1996.
- [8] J.M. Huntley, “Three-dimensional Noise-immune Phase Unwrapping Algorithm,” *Applied Optics*, vol. 40, pp. 3901-3908, 2001.
- [9] P. Soille, *Morphological Image Analysis: Principles and Applications*, Springer-Verlag, 1999. (pp. 173-174)
- [10] A. Ng, M. Jordan, Y. Weiss, “On Spectral Clustering: Analysis and an Algorithm,” *NIPS*, 2002.
- [11] M. Brand, K. Huang, “A Unifying Theorem for Spectral Embedding and Clustering,” *AISTATS*, 2003.
- [12] Y. Cheng, “Mean Shift, Mode Seeking, and Clustering,” *IEEE Transactions on Pattern Analysis and Machine Intelligence*, vol. 17, no. 8, 1995.
- [13] P. Yee, S. Haykin, “Pattern Classification as an Ill-posed, Inverse Problem: a Regularization Approach,” *ICASSP*, pp. I-597–600, 1993.